7-14-2023

Dosimetric significance of manual density overrides in oropharyngeal cancer

Thomas Lo Greco
Grand Valley State University

Dosimetric significance of manual density overrides in oropharyngeal cancer

Thomas G. Lo Greco

Medical Dosimetry Graduate Program, Grand Valley State University

ABSTRACT

Kilovoltage computed tomography plays a crucial role in radiotherapy planning. However, the presence of high-density metallic objects can introduce streaking artifacts in CT scans, resulting in inaccurate dose calculations by the treatment planning software. Previous studies have explored manual density overrides and artifact reduction algorithms individually to enhance dose calculation accuracy, but their combined application on patient plans within a treatment planning system remains unexplored.

This research aims to assess the necessity of manual density overrides when an artifact reduction algorithm is already employed to address dental artifacts in oropharyngeal cancer treatment plans. A total of 20 previously treated volumetric modulated arc therapy plans were collected, and manual density overrides were removed followed by plan recalculation. Dosimetric parameters were then compared between the original and modified plans.

Statistical analysis revealed several dosimetric parameters for the planning target volume (PTV), clinical target volume (CTV), and oral cavity that exhibited statistically significant differences upon removing the manual density override. However, these differences were found to be small in absolute terms. No other organs evaluated demonstrated statistically significant differences in dose. The most significant disparity observed was an 8.26 cGy increase in mean dose to the CTV, which represents only 0.12% of the prescription dose.

Based on these findings, it can be concluded that manual density overrides are likely unnecessary when an artifact reduction algorithm is employed in oropharyngeal cancer cases.

Keywords: Metal artifact reduction algorithm, manual density override, oropharyngeal cancer, head and neck cancer, dental artifacts

INTRODUCTION

Kilovoltage computed tomography (KV CT) scans are used as a starting point for planning external beam radiotherapy (EBRT). They allow for optimal tissue visualization, contouring, and radiation dose modeling. Modern day CT machines perform helical scanning, meaning that the patient is moved through the bore of the machine while an internal gantry consisting of an x-ray tube and an image receptor array arranged 180 degrees apart continuously rotates around the patient. The resulting data is reconstructed into a viewable image via a filtered backprojection algorithm and is displayed in voxels, which are similar to pixels, but with the addition of the third dimension. Each individual voxel has its own distinct grayscale level that corresponds to the linear attenuation coefficient of the tissue the x-ray beam traverses and the corresponding radiodensity of that tissue. That grayscale value is the Hounsfield Unit (HU) named after Sir Godfrey Hounsfield, who is credited with the development of computed tomography. The baseline HU value of 0 is assigned to distilled water at standard temperature and pressure; all other values are relative to the 0 value. As tissue becomes denser the HU values increase, and as tissue becomes less dense the values decrease. Metals can be upwards of 4000+ HU, dense bone is around 1000 HU, soft tissue is roughly 30 HU, adipose tissue is close to -80 HU, and air is -1000 HU (Washington et al., 2021).

Once a patient is prescribed a course of radiation, they begin with a KV CT in the CT simulation room. The CT machines that are used for radiotherapy planning are equipped with a flat carbon fiber table to limit as much radiation interaction with the table as possible, as carbon fiber has a very low linear attenuation coefficient. The patient is positioned in the same way that they will be for treatment and instructed by the radiation therapists regarding the specific imaging protocols. The patient is then scanned, along with the positioning devices. An issue can

arise in the treatment planning process when a patient has a high-density implant in their body: it creates what is called an artifact. The artifact is caused by incorrect reconstruction of the data due to the high-density material and it appears as a streaking density across the CT plane. These artifacts are not a true representation of the patient's anatomy, and thus will lead to erroneous dose calculations. The artifact, whether it appears as a positive or negative density, will then be converted by the treatment planning software (TPS) into an electron density. The electron density of the tissue is the way a TPS models radiation interactions and allows for modern radiotherapy techniques to be applied (Sudhyadhom, 2020). If the TPS converts the artifact into electron densities, the assumption is then that the artifact is part of the patient, and therefore it will model radiation interactions based on the purported density of that tissue.

To prevent this inaccurate dose calculation, an orthopedic metal artifact reduction (OMAR) algorithm can be used to reduce the impact of the inaccurate reconstruction to create an image that exists much closer to the patient's true anatomy. The OMAR algorithm is most often used for the spine, hip, and head and neck treatment areas. If an OMAR scan is necessary, one will be generated and sent to the dosimetrist. The OMAR scan is then used to plan the patient's course of radiation.

An OMAR algorithm is an iterative algorithm based on the original filtered backprojection algorithm, meaning that it performs its function repeatedly and with each repetition the effect of the artifact is further reduced (Sillanpaa et al., 2020). The OMAR algorithm, as its name suggests, was originally intended to reduce the artifact of orthopedic implants. Orthopedic implants found in the spine and hip have a relatively low atomic number compared to that of dental amalgam, as most orthopedic implants are composed of stainless steel, titanium alloys, and CoCrMo alloys (Merola & Affatato, 2019), while dental amalgam,

also called dental fillings or silver fillings, according to the FDA is composed of approximately

50% elemental mercury along with a silver, tin, and copper alloy (Health, 2021). The atomic

numbers for the most common elements in orthopedic implants are as follows: Titanium: 22,

Cobalt: 27, Chromium: 24, Nickel: 28, Aluminum: 13, Carbon: 6, Manganese: 25, Phosphorus:

15, Sulfur: 16, and Silicon: 14 (*The Elements of Steel | American Experience | PBS*, n.d.), while

the atomic number for Mercury is 80, Silver is 47, Tin is 50, and copper is 29. Since the atomic

number of the major component of dental amalgam is significantly higher than elements used in

orthopedic implants, the linear attenuation coefficient will likewise be much higher, leading to a

more pronounced artifact presence (Boas & Fleischmann, 2012; Priamo, 2014).

OMAR algorithms are excellent tools, though they are not perfect, and a manual density

override may still be necessary if a patient is found to have significant artifact from high density

implants. A manual density override consists of a visual and HU based assessment and

segmentation of the affected area, which is then contoured in the TPS and given a density

override. This allows the TPS to treat the delineated areas of artifact as though they had a

homogenous density, most often of water or soft tissue, with HUs of 0-30, respectively.

It is of the utmost importance to ensure accurate treatment planning and delivery,

especially in head and neck cancers, as these radiotherapy patients can experience debilitating

side effects from treatment. To compound the problem, many of these patients have amalgam

fillings or other dental prostheses that cause significant artifacts and could influence the dose

deposition to surrounding structures. As a consequence of the helical scanning process, the

artifact's effect will be most pronounced along the axial slices on which the offending appliance

is found, and several slices superior and inferior to its maximum extent, which in the case of

dental appliances is the oral cavity and oropharynx. The oral cavity includes and is anterior to the

retromolar trigone, the anterior two thirds of the tongue, the hard palate, the gums, the lips, the buccal mucosa, the teeth, and the floor of the mouth. The oropharynx includes the posterior third of the tongue, the soft palate, the palatine and lingual tonsils, and the lateral and posterior walls of the pharynx between the soft palate superiorly and the epiglottis inferiorly (American Cancer Society, 2021). Organs at risk for an overdose include the parotids, submandibular glands, spinal cord, esophagus, larynx, and bilateral cochleas. The artifact correction performed via OMAR and manual density override in head and neck cancers is commonplace and therefore leads to the question of whether the manual correction significantly improves the dose calculation accuracy over an OMAR correction alone.

LITERATURE REVIEW

Much research has delved into the benefits of using OMAR scans versus uncorrected scans for treatment planning, and how it shows a marked benefit for contouring accuracy and the accuracy of the planned treatment versus the treatment delivered (Sillanpaa et al., 2020). Sillanpaa et al. concluded that OMAR improves tissue delineation and contouring, but that there was no significant change in tissue dose when comparing OMAR and uncorrected scan treatments, though cold spots were less severe with OMAR corrected scans.

A study by Nielsen et al. compares OMAR versus KerMAR (another artifact correction algorithm) versus manual override benefits for normal tissues doses, though none of them combined, and again found no significant benefit to normal tissues, and even stated a negative influence on dose calculations from manual override alone (Nielsen et al., 2019). Another study found that OMAR corrected scans are superior to manual contour corrected scans because it reduces interobserver variability allowing for more consistency (Koike et al., 2020), however this study compares static IMRT field treatment plans, which are not the commonplace practice

any longer. An additional study used thirteen CT scans from the Cancer Imaging Archive, on which they fabricated multiple different orientations of dental fillings and compared manual density override with a GAN-MAR algorithm and found that the algorithm was superior to the manual override regarding structural similarity to the reference CT (Nakamura et al., 2021).

The vast majority of research surrounding corrected scans features investigations of the algorithm used to correct a scan compared to the scan without any correction, or a manual correction alone rather than a combination of algorithm correction with a manual override. The research is quite clear that an algorithmic correction is superior to manual contour correction in the accuracy of dose modeling and tissue delineation. The sum of research also shows a modest change in dose to organs at risk (OAR) and target structures when comparing uncorrected to a single method of correction.

There is a limited volume of research that investigates how OMAR corrected scans combined with manual density correction differs from OMAR corrected only scans, but the research approaches the investigation using phantoms rather than actual patients (Emberru, 2021). The study evaluated the dose received in the oral cavity alone and used dual energy CT scans (kV and MV) to better delineate the actual high-density material, which is not available in many clinics, though it is more accurate. The research also used a twelve-beam arrangement, which is not a commonly utilized treatment beam arrangement. Emberru et al used diodes to directly measure the dose received in the areas of interest, as opposed to relying on computer modeling, which is more accurate, though not practical on actual patients.

There is a lack of research surrounding the commonplace practice of using OMAR corrected scans with the addition of manual density override of dental artifacts that remain, and how much benefit is received by the patient, especially for oropharyngeal cancers. Dental

artifacts are likely to have some of the greatest effect on actual dose distribution in this area due to helical scanning as previously discussed. The purpose of this study is to quantitatively evaluate the change in dose to the targets and OARs with the use of an OMAR corrected CT scan combined with a manual density override as compared to an OMAR alone correction, in order to ascertain whether or not the additional manual density overrides provide clinically significant benefit to the patient.

MATERIALS AND METHODS

The purpose of this study was to quantitatively evaluate the impact of using a manual density override in conjunction with an OMAR-corrected CT scan on dose to targets and organs at risk (OAR). This retrospective study evaluated 20 randomly selected volumetric modulated arc therapy (VMAT) oropharyngeal cancer treatment plans that were planned and treated between 2019 and 2023 at a Midwest radiation oncology clinic. The study underwent the IRB process and received approval from both the Grand Valley State University IRB and the Midwest radiation oncology clinic IRB.

The inclusion criteria for the selected plans were as follows: VMAT plans with 2-3 full arcs that were approved by a physician, collimator angles between 15° and 90°, beam energies of 6MV, prescription dose of 7000cGy in 35 fractions, an isocentric setup on Varian Linacs (either TrueBeam or Trilogy), inclusion of amalgam fillings and/or dental implants (referred to as dental appliance), use of both OMAR algorithm and manual density override contours, between 1 and 12 dental appliances in the plan, PTV overlapping the density override in the inferosuperior direction by at least one slice, GTV overlapping the 1 cm superioinferior region of the density override by at least one slice, at least 95% of the PTV volume being covered by the prescription

dose, and the volume of the density override being between 2cc and 70cc. Plans that did not meet these inclusion criteria were excluded from the study.

The original contours were created by three different dosimetrists and four different physicians, which reduced the potential for bias from a single individual contouring or approving the structures or plan. Dental appliances were contoured using an HU-specific selection tool and were limited to the non-native material. Manual density overrides were segmented using a brush tool via visual analysis of the artifact (see figures 1 and 2). All manual density overrides were assigned an HU value of either water or soft tissue (density of 1.000 g/cm^3), and the dental appliance volume was subtracted from the manual density override structure to ensure that there was no overlap between the two. Each manual override was inspected by the researcher to ensure that it met the contouring specifics and inclusion criteria by evaluating the dental appliance with a bone window (level 450, window 1600) to ensure relative homogeneity among the override contours.

The CT scans were performed with helical scans at a department standard of 120 kVp and a variable mAs depending on patient size, with 3mm slice thickness, a 512 x 512 matrix size, and a FOV of 80cm. Only OMAR scans were used for planning, thereby further reducing interobserver variance regarding manual density override volumes. All plans were created on Raystation TPS for TrueBeam or Trilogy Varian Linacs. The evaluation of the original plan compared to the plan without the density override all took place on Raystation version 10A SP1 with collapsed cone v5.3 calculation algorithm. If the machine parameter models were out of date from the most recent model, the plans were recalculated with the current machine model without changing any machine parameters or rescaling of MUs prior to removing the density override to control for variance of machine model parameters.

Two plans were used for comparison in this study. The original plans were created on an OMAR-corrected CT scan with an additional manual density override correction contour. The researcher then removed the manual density override correction contour from the scan and recalculated the plan without changing any machine parameters and the MUs were not rescaled.

The effect of removing the override structure was evaluated by comparing the mean, maximum (D0.01cc), and minimum (D100%) doses of the PTV, GTV, CTV, parotids, submandibular glands, spinal cord, and oral cavity before and after override removal. The target doses were evaluated within a limited geometric range of 1 cm (or the next furthest slice location) inferiosuperior to the maximum extent of the density override to reduce dilution of significance due to a volumetric effect, and the target volumes were edited to not extend outside of this range. Only the 7000cGy PTV, CTV, and GTV were evaluated when multiple dose levels were present. In addition to dose, the PTV was also evaluated for dose homogeneity, conformality, and the volume receiving 105% of the prescription dose (V105). The values of the original plans were compared to the modified plans based on the volume of the manual override and the distance between the geometric center of the cropped target volume or OAR and the geometric center of the density override. The spinal cord distance was evaluated based on the closest distance between the edge of the spinal cord structure and the edge of the density override structure as opposed to the geometric center of both, which would yield a truer representation of their proximity. The doses to the PTV and oral cavity were additionally evaluated based on the volume of overlap with the density override as these two structures were the ones most likely to overlap with the density override volume.

To create the modified regions of interest (ROIs) for the targets, the upper and lower borders of the artifact were denoted and the next slice beyond 1cm above and below was

contoured. The structure was then interpolated and named "limited structure." An ROI algebra

was used to create PTV, CTV, and GTV contours that were only within that limited region

structure, thereby creating evaluation structures to reduce a volumetric dilution effect. The area

within the limited region structure that received 7000 cGy was used to evaluate the conformality

index, along with the volume of the PTV evaluation structure. The remainder of the dose

parameters were collected via clinical goal inputs in Raystation. To ascertain the distance

between the geometric center of the ROIs and the density override structure a script was written

to compare the three dimensional coordinates of each ROI and the manual density override as

follows: $distance = \sqrt{(x2 - x1)^2 + (y2 - y1)^2 + (z2 - z1)^2}$.

A one way within factor ANOVA test with a constant covariate was performed to assess

for significance. The assumption of sphericity was tested and met. The lines of best fit were

compared for the respective data sets with the override present, and without the override present,

and the lines of best fit were compared. The covariate changes between analyses (distance from

center, volume of density override, etc.) but is constant within the independent factor of the

presence of an override. A *p* value of 0.05 or less was considered statistically significant. All

statistical analysis was performed using SAS software.

RESULTS

The average mean, minimum, and maximum doses for all structures of interest, as well as

the HI, CI, and V105 for the PTV with and without the override are summarized in Table 1.

Additionally, all the results for the one way within factor ANOVA test with a constant covariate

are condensed on Table 2. For results that have a failed to meet the criteria of statistical

significance (*p* value of less than 0.05), the null hypothesis was unable to be rejected and it was

concluded that the average dosimetric parameter for the structure with an override was not

different from the average dosimetric parameter for the structure without an override. The results that did show statistical significance, and the accompanying confidence intervals, are reported for each structure in greater detail. The average distance between the centers of the structures and the center of the density override, the average density override volume, and the average volume of overlap with the density override are summarized in Table 3.

PTV

When evaluating the average mean dose, using the volume of the density override as a covariate, the average mean dose for the PTV with an override was different from the average mean dose for the PTV without an override ($t(18) = 2.65$, p value $= 0.0164$). For every 1cc increase in the volume of the density override, the average mean dose decreased by 0.4455 cGy for the PTV with a density override, while for the PTV without a density override, the average mean dose decreased by 0.5396 cGy. There is 95% confidence that for every 1cc increase in the volume of the density override the average mean dose is between 0.01943 cGy and 0.1688 cGy smaller for the PTV without an override than for the PTV with an override.

With the volume of overlap between the density override and the PTV as a covariate, the average mean dose for the PTV with an override was different from the average mean dose for the PTV without an override ($t(18) = 4.18$, p value $= 0.0006$). For every 1cc increase in the volume of overlap between the density override and the PTV, the average mean dose increased by 4.04503 cGy for the PTV with a density override, while for the PTV without a density override, the average mean dose increased by 3.0161 cGy. There is 95% confidence that for every 1cc increase in the volume of overlap between the density override and the PTV the average mean dose is between 0.5115 cGy and 1.5464 cGy smaller for the PTV without an override than for the PTV with an override .

For the average CI, with the volume of overlap between the density override and the PTV as a covariate, the average CI for the PTV with an override was different from the average CI for the PTV without an override ($t(18) = 3.56$, p value = 0.0022). For every 1cc increase in the volume of overlap between the density override and the PTV, the average CI increased by 0.00479 for the PTV with a density override, while for the PTV without a density override, the average CI increased by 0.002979. There is 95% confidence that for every 1cc increase in the volume of overlap between the density override and the PTV the average CI is between 0.000743 and 0.002883 smaller for the PTV without an override than for the PTV with an override.

In summary, when evaluating the average volume of the density override, when the density override is removed from a plan the average mean dose will decrease by between 0.53 cGy and 4.68 cGy. When evaluating the average volume of overlap between the density override and the PTV, when the density override is removed, the average mean dose will decrease by between 0.64 cGy and 1.93 cGy, and the average CI will decrease by between 0.0009 and 0.0036.

CTV

When analyzing the average mean dose of the CTV, when using the distance between the center of the density override and the center of the CTV as a covariate, the average mean dose for the CTV with an override was different from the average mean dose for the CTV without an override ($t(18) = -2.23$, p value = 0.0383). For every 1cm increase in the distance between the center of the density override and the center of the CTV, the average mean dose decreased by 1.57857 cGy for the CTV with a density override, while for the CTV without a density override, the average mean dose decreased by 0.7815 cGy . There is 95% confidence that for every 1cm increase in the distance between the center of the density override and the center of the CTV the

average mean dose is between 0.04779 cGy and 1.5463 cGy larger for the CTV without an override than for the CTV with an override.

With the volume of the density override as a covariate, the average mean dose for the CTV with an override was different from the average mean dose for the CTV without an override ($t(18) = 2.23$, p value = 0.0389). For every 1cc increase in the volume of the density override, the average mean dose decreased by 0.52965 cGy for the CTV with a density override, while for the CTV without a density override, the average mean dose decreased by 0.6064 cGy. There is 95% confidence that for every 1cc increase in the volume of the density override the average mean dose is between 0.004364 cGy and 0.1492 cGy smaller for the CTV without an override than for the CTV with an override.

Overall, when evaluating the average distance between the CTV and the density override, when the density override is removed, the average mean dose for the CTV will increase by between 0.26 cGy and 8.26 cGy. When evaluating the average volume of the density override, when the density override is removed the average mean dose for the CTV will decrease by between 0.12 cGy and 4.10 cGy.

ORAL CAVITY

For the average mean dose, with the distance between the center of the density override and the center of the oral cavity as the covariate, the average mean dose for the oral cavity with an override was different from the average mean dose for the oral cavity without an override ($t(18) = -2.50$, p value = 0.0221). For every 1cm increase in the distance between the center of the density override and the center of the oral cavity, the average mean dose increased by 80.4462 cGy for the oral cavity with a density override, while for the oral cavity without a density override, the average mean dose increased by 81.8935 cGy. There is 95% confidence that

for every 1cm increase in the distance between the center of the density override and the center of the oral cavity the average mean dose is between 0.2329 cGy and 2.6616 cGy larger for the oral cavity without an override than for the oral cavity with an override.

With the volume of the density override as a covariate, the average mean dose for the oral cavity with an override was different from the average mean dose for the oral cavity without an override ($t(18) = 2.59$, p value $= 0.0186$). For every 1cc increase in the volume of the density override, the average mean dose increased by 3.1366 cGy for the oral cavity with a density override, while for the oral cavity without a density override, the average mean dose increased by 3.0762 cGy. There is 95% confidence that for every 1cc increase in the volume of the density override the average mean dose is between 0.0114 cGy and 0.1094 cGy smaller for the oral cavity without an override than for the oral cavity with an override.

With the volume of overlap between the density override and the oral cavity as a covariate, the average mean dose for the oral cavity with an override was different from the average mean dose for the oral cavity without an override ($t(18) = 2.96$, p value $= 0.0083$). For every 1cc increase in the volume of overlap between the density override and the oral cavity, the average mean dose decreased by 24.5887 cGy for the oral cavity with a density override, while for the oral cavity without a density override the average mean dose decreased by 24.7990 cGy. There is 95% confidence that for every 1cc increase in the volume of overlap between the density override and the oral cavity the average mean dose is between 0.0613 cGy and 0.3592 cGy smaller for the oral cavity without an override than for the oral cavity with an override.

When analyzing the mean minimum dose, with the volume of overlap between the density override and the oral cavity as a covariate, the mean minimum dose for the oral cavity with an override was different from the mean minimum dose for the oral cavity without an

override ($t(18) = 2.58$, p value $= 0.0188$). For every 1cc increase in the volume of overlap between the density override and the oral cavity, the mean minimum dose decreased by 39.4125 cGy for the oral cavity with a density override, while for the oral cavity without a density override, the mean minimum dose decreased by 39.7165 cGy. There is 95% confidence that for every 1cc increase in the volume of overlap between the density override and the oral cavity the mean minimum dose is between 0.0565 cGy and 0.5515 cGy smaller for the oral cavity without an override than for the oral cavity with an override.

In summary, when evaluating the average distance between the density override and the oral cavity, when the density override is removed, the average mean dose will increase by between 0.36 cGy and 4.13 cGy. When evaluating the average volume of the density override, when the density override is removed, the average mean dose will decrease by between 0.31 cGy and 3.01 cGy. When evaluating the average volume of overlap between the density override and the oral cavity, when the density override is removed, the average mean dose will decrease by between 0.47 cGy and 2.73 cGy, and the mean minimum dose will decrease by between 0.43 cGy and 4.19 cGy.

DISCUSSION

The use of OMAR scans to improve dose calculation accuracy is important in oropharyngeal cancer, especially considering the significant artifacts produced by dental appliances. However, the combined use of OMAR scans and manual density overrides had yet to be thoroughly investigated in patient plans. In this study the effects of manual density overrides were examined to establish their necessity, or lack thereof, in oropharyngeal cancer when an OMAR algorithm is used. The results indicate statistical significance in some instances, while overall the change is small in absolute terms.

The only structures that showed any statistically significant differences in dose when the density override was removed were the PTV, CTV, and oral cavity. For the PTV there was, at most, a 4.68 cGy decrease in the mean dose, and the CI decreased by, at most, 0.0036. There were no other statistically significant changes for the PTV. A possible explanation for the decrease in dose and CI would be the inherent photon absorption of areas on the scan deemed to have a higher electron density – the previously overridden volume – thereby decreasing the dose deposited in the shadow of the higher density volume.

The CTV showed conflicting results. There was, at most, an 8.26 cGy decrease in the mean dose when evaluating the distance between the CTV and the density override. However, when evaluating the volume of the density override there was an average increase in mean dose of, at most, 4.10 cGy. The cause of this incongruence could be due to the variation in the location of the CTV within the oropharynx.

The oral cavity was, by far, the most affected structure, but it too showed conflicting results. When examining the distance between the structures there was, at most, a 4.13 cGy increase in mean dose, but when evaluating the volume of the density override there was, at most, a 3.01 cGy decrease in mean dose. When using the volume of overlap as a covariate, there was, at most, a decrease in the mean dose of 2.73 cGy and decrease in the minimum dose of 4.19 cGy. A likely cause of the conflicting results could be the physically close nature of the oral cavity and density override volumes, thereby making the distance between the geometric centers more susceptible to small changes in the shape of the density override volume, such as when the artifact streaks across the axial plane. Smaller changes in this distance can represent a much larger percentile change than for two structures which are further apart.

These results are statistically significant, as previously reported, but the clinical relevance of even the largest change, 8.26 cGy, is extremely limited; in these cases, the patient is receiving a prescription dose of 7000 cGy with average mean doses ranging up to 7212.20 cGy. This means that at most there is a 0.12% change in the mean dose (see figure 3). This indicates that contouring manual density overrides on OMAR scans is likely unnecessary in the case of oropharyngeal cancers.

This lack of difference between the doses calculated on the OMAR scan and the OMAR plus manual density override scan can be explained by the accuracy of the OMAR algorithm, as discussed earlier and as discussed in the literature. It uses an iterative method based on the original filtered backprojection algorithm. These algorithms are far more efficient and accurate in reducing the effect of an artifact than any manual contour can be. As accurate at the OMAR scans are, even they show only a modest change in dose deposition (Sillanpaa et al., 2020), so it stands to reason that a necessarily more inaccurate manual contour would have even less of an effect.

Previous studies showed a mild improvement in dose deposition when some form of algorithmic density correction is used, and some even showed a negative impact when manual density overrides were used. This study's results show that a combination of algorithmic correction and manual correction yields no significant change in dose deposition.

This study has several strengths. This study aims to control for three of the most likely causes for change in dose and evaluates the changes with respect to each individual covariate. This allows for individual assessment of the likelihood of a change in the dose as each individual case may require. This study also shows the change in dose per unit change of the covariate, further allowing for case-by-case assessment. This study also attempts to average interobserver

variance by using contours made by multiple dosimetrists and physicians, reducing the impact of a single contour skewing the data.

The study possesses several inherent limitations, one of which pertains to its sample size. Specifically, the current study's inclusion of only 20 cases results in constrained statistical power. Future studies should attempt to include a greater number of cases. Additionally, there may be a difference in the final plans if the manual density override is never introduced into the equation. The planner may evaluate structures differently based on the change in dose deposition and optimize accordingly.

This research suggests there is no need to contour artifacts from dental appliances and perform manual density overrides in the case of oropharyngeal cancer treatment when an OMAR scan is used. An area for future research would be creating plans on the same scan, one without the override and one with the override, for comparison, as opposed to removing the override and recalculating.

CONCLUSION

When treating oropharyngeal cancer, the combination of a manual density override and an OMAR correction does affect the dose deposition in the PTV, CTV, and oral cavity compared to using an OMAR correction alone. However, the impact of this combined approach is so minor that it is unlikely to have any clinical significance, as the largest difference was a change of 0.12% of the prescription dose. Furthermore, the doses to the remaining OARs did not show any statistically significant change.

Therefore, manual density overrides for dental artifacts in the case of oropharyngeal cancer when an OMAR scan is used may be unnecessary. Foregoing this step during treatment

planning would help to reduce treatment planning time and increase standardization by reducing interobserver variability.

CONFLICTS OF INTEREST

ACKNOWLEDGEMENTS

References

American Cancer Society. (2021, March 23). *What Are Oral Cavity and Oropharyngeal*

   Cancers? American Cancer Society. https://www.cancer.org/cancer/oral-cavity-and-

   oropharyngeal-cancer/about/what-is-oral-cavity-cancer.html

Boas, F. E., & Fleischmann, D. (2012). CT artifacts: Causes and reduction techniques. *Imaging*

   in Medicine, *4*(2), 229–240. https://doi.org/10.2217/iim.12.13

Emberru, M. (2021). Assessment Of A Treatment Planning Protocol For The Reduction Of

   Dosimetry Calculation Errors In Radiotherapy For Head And Neck Patients With Dental

   Implants. *McMaster University*, 97.

Health, C. for D. and R. (2021, February 18). *Dental Amalgam Fillings*. FDA; FDA.

   https://www.fda.gov/medical-devices/dental-devices/dental-amalgam-fillings

Koike, Y., Anetai, Y., Takegawa, H., Ohira, S., Nakamura, S., & Tanigawa, N. (2020). Deep

   learning-based metal artifact reduction using cycle-consistent adversarial network for

   intensity-modulated head and neck radiation therapy treatment planning. *Physica Medica*,

   78, 8–14. https://doi.org/10.1016/j.ejmp.2020.08.018

Merola, M., & Affatato, S. (2019). Materials for Hip Prostheses: A Review of Wear and Loading

   Considerations. *Materials*, *12*(3), 495. https://doi.org/10.3390/ma12030495

Nakamura, M., Nakao, M., Imanishi, K., Hirashima, H., & Tsuruta, Y. (2021). Geometric and

   dosimetric impact of 3D generative adversarial network-based metal artifact reduction

   algorithm on VMAT and IMPT for the head and neck region. *Radiation Oncology*, *16*(1).

   https://doi.org/10.1186/s13014-021-01827-0

Nielsen, J. S., Van Leemput, K., & Edmund, J. M. (2019). MR-based CT metal artifact reduction

    for head-and-neck photon, electron, and proton radiotherapy. *Medical Physics*, *46*(10),

    4314–4323. https://doi.org/10.1002/mp.13729

Priamo, F. (2014, November 5). *Linear attenuation coefficient | Radiology Reference Article |*

    Radiopaedia.org. Radiopaedia. https://doi.org/10.53347/rID-31918

Sillanpaa, J., Lovelock, M., & Mueller, B. (2020). The effects of the orthopedic metal artifact

    reduction (O-MAR) algorithm on contouring and dosimetry of head and neck

    radiotherapy patients. *Medical Dosimetry*, *45*(1), 92–96.

    https://doi.org/10.1016/j.meddos.2019.07.003

Sudhyadhom, A. (2020). On the molecular relationship between Hounsfield Unit (HU), mass

    density, and electron density in computed tomography (CT). *PLoS ONE*, *15*(12),

    e0244861. https://doi.org/10.1371/journal.pone.0244861

The Elements of Steel | American Experience | PBS. (n.d.). Retrieved October 25, 2022, from

    https://www.pbs.org/wgbh/americanexperience/features/streamliners-steel/

Washington, C., Leaver, D., & Trad, M. (2021). *Principles and Practice of Radiation Therapy*

    (Fifth). Elsevier.

APPENDIX

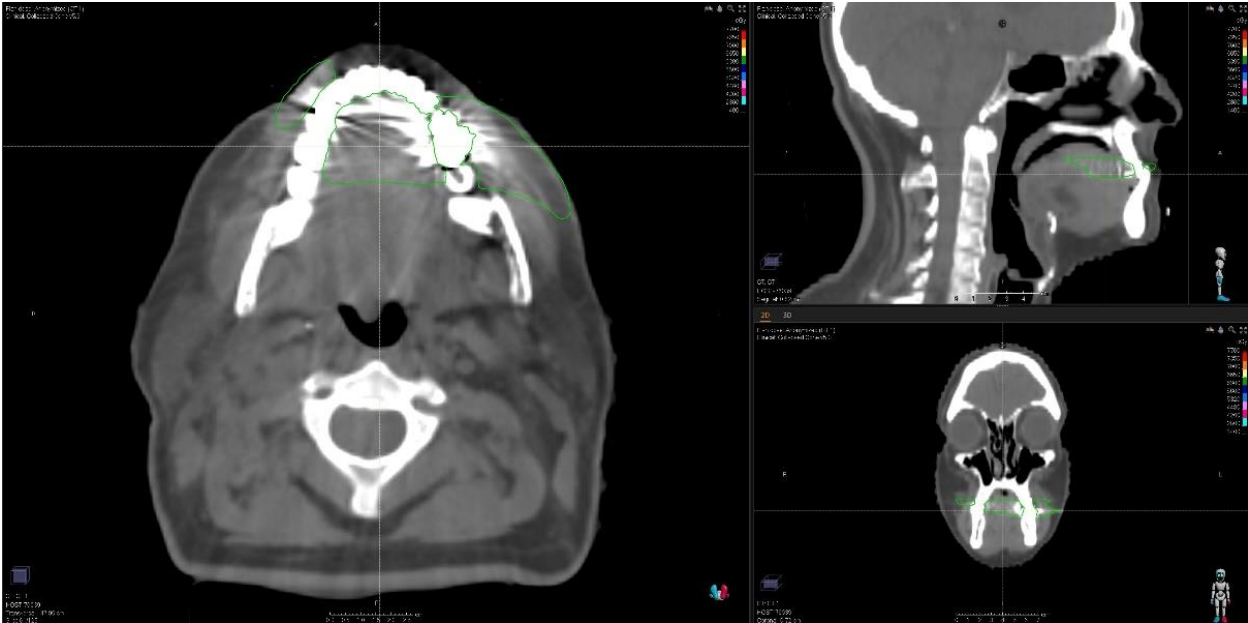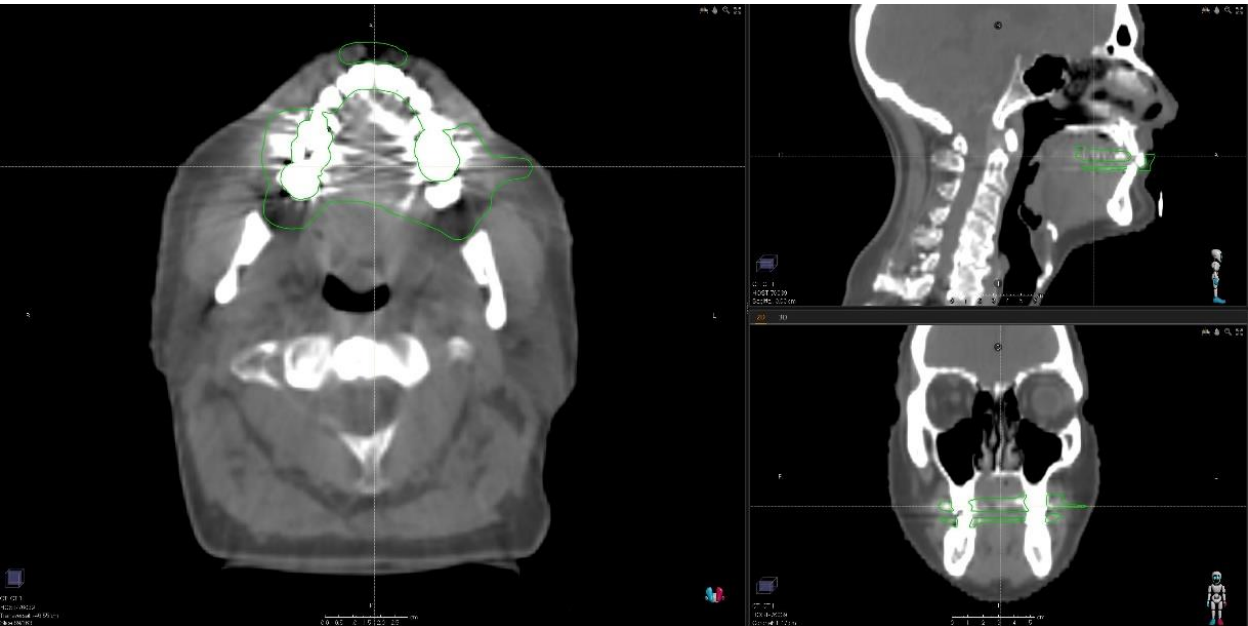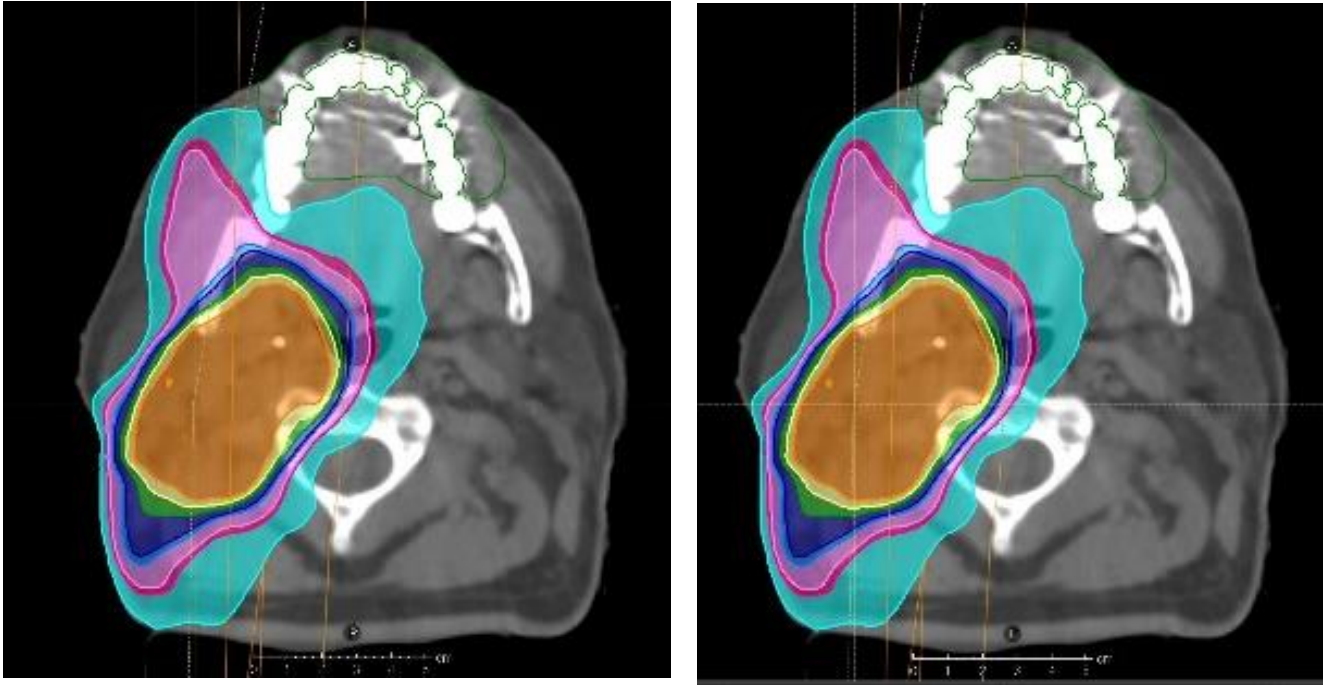*Figure 1:Manual density override contoured around dental appliances.*

Figure 2: Manual density override contoured around dental appliances.

Figure 3: Dose distribution with the override present (left) and dose distribution after the override is removed and the plan is recalculated (right).

Table 1: Dosimetric Parameters for structures of interest with and without the density override.

Dosimetric Parameters for structures of interest with and without the density override

Structure Parameter	With Override		Without Override	
PTV	Average	SD	Average	SD
Mean (cGy)	7188.25	115.25	7185.85	114.84
Min (cGy)	5530.15	984.46	5526.50	984.49
Max (cGy)	7480.90	149.30	7480.60	149.28
HI	0.74	0.13	0.74	0.13
CI	1.07	0.15	1.07	0.15
V105 (cc)	11.37	23.20	11.17	22.82
CTV				
Mean (cGy)	7212.20	110.13	7210.20	109.56
Min (cGy)	6736.75	326.56	6732.45	325.65
Max (cGy)	7467.65	148.85	7468.90	147.62
GTV				
Mean (cGy)	7198.20	104.59	7197.20	103.95
Min (cGy)	7013.85	117.99	7010.20	119.23
Max (cGy)	7406.20	152.90	7406.30	153.23
Left Parotid				
Mean (cGy)	2034.50	969.94	2034.30	969.82
Min (cGy)	507.75	282.15	507.75	282.09
Max (cGy)	5955.85	1942.93	5955.30	1943.06
Right Parotid				
Mean (cGy)	2011.50	632.97	2010.80	632.48
Min (cGy)	508.35	231.38	508.40	231.39
Max (cGy)	6253.40	1237.35	6249.70	1237.84
Left Submandibular				
Mean (cGy)	5580.20	1914.08	5580.35	1913.96
Min (cGy)	4331.60	2125.75	4331.60	2125.57
Max (cGy)	6581.95	1492.81	6583.70	1492.11
Right Submandibular				
Mean (cGy)	5375.65	1624.41	5375.90	1624.51
Min (cGy)	4202.10	1981.17	4202.25	1981.16
Max (cGy)	6730.50	1036.36	6729.05	1036.45
Spinal Cord				
Mean (cGy)	1443.40	349.45	1443.30	349.40
Min (cGy)	19.45	17.61	19.45	17.61
Max (cGy)	3506.90	458.59	3508.35	458.98
Oral Cavity				
Mean (cGy)	2484.95	565.93	2482.85	565.33
Min (cGy)	1017.60	415.51	1016.20	416.80
Max (cGy)	5752.75	831.97	5745.75	827.80

Table 2: One way within factor ANOVA test with a constant covariate with results for each covariate. Statistically significant p *values are in bold.*

One way within factor ANOVA test with a constant covariate results for each covariate

Structure Parameter	Distance from the center		Volume of Density Override		Volume of Overlap	
PTV	t-value	p-value	t-value	p-value	t-value	p-value
Mean	-2.01	0.05970	2.65	**0.0164**	4.18	**0.0006**
Min	-0.17	0.48710	1.24	0.2324	2.01	0.0596
Max	0.29	0.77770	-1.17	0.2578	-1.86	0.0791
HI	-0.25	0.80920	1.05	0.3078	1.88	0.0764
CI	-1.41	0.17430	1.69	0.1081	3.56	**0.0022**
V105	-0.93	0.36380	1.80	0.0886	0.96	0.3474
CTV						
Mean	-2.23	**0.03830**	2.23	**0.0389**		
Min	-1.06	0.30370	0.75	0.4614		
Max	0.57	0.57840	-0.99	0.3363		
GTV						
Mean	-2.03	0.05750	0.84	0.4093		
Min	-0.39	0.70330	0.79	0.4415		
Max	0.56	0.58550	-1.55	0.1374		
Left Parotid						
Mean	-0.31	0.76350	1.51	0.1493		
Min	1.12	0.27750	0.98	0.3378		
Max	-1.47	0.15990	-0.10	0.9241		
Right Parotid						
Mean	-1.65	0.11600	1.63	0.1201		
Min	1.30	0.20850	-1.69	0.0662		
Max	-1.97	0.06390	1.17	0.2583		
Left Submandibular						
Mean	-0.20	0.84140	-0.53	0.6048		
Min	0.44	0.66820	-0.69	0.5000		
Max	1.32	0.20310	0.20	0.8468		
Right Submandibular						
Mean	1.16	0.25980	-1.36	0.1907		
Min	0.73	0.47360	-0.55	0.5899		
Max	-0.77	0.44870	1.64	0.1187		
Spinal Cord						
Mean	-0.16	0.87220	1.33	0.2007		
Min	DNC	DNC	DNC	DNC		
Max	-1.15	0.26690	0.37	0.7152		
Oral Cavity						
Mean	-2.50	**0.02210**	2.59	**0.0186**	2.96	**0.0083**
Min	-0.65	0.52100	0.62	0.5407	2.58	**0.0188**
Max	-0.13	0.89880	1.32	0.2048	0.92	0.3675

*DNC = models did not converge

Table 3: Covariate Averages

Covariate Averages

Covariate	Average
Distance from the center of density override (cm)	
PTV	5.34
CTV	5.34
GTV	5.51
Left Parotid	8.67
Right Parotid	8.71
Left Submandibular	6.58
Right Submandibular	6.63
Spinal Cord	4.91
Oral Cavity	1.55
Volume of Density Override (cc)	27.47
Volume of Overlap with density override (cc)	
PTV	1.25
Oral Cavity	7.60